International Journal of Nanoelectronics and Materials
IJNeaM
ISSN 198-5761 | E-ISSN 2232-1535

Dielectrophoresis as an Adjunctive Technique for Fibroblast Cell Migration to Enhance Wound Closure

Nur Nasyifa Mohd Maidin[a], Revathy Deivasigamani[a], Muhamad Ramdzan Buyong[a], Ruslinda A. Rahim[b,c] and Mohd Ambri Mohamed[a,*]

[a]*Institute of Microengineering and Nanoelectronics (IMEN), Universiti Kebangsaan Malaysia (UKM), 43000 Bangi, Malaysia.*
[b]*Institute of Nano Electronic Engineering (INEE), Universiti Malaysia Perlis (UniMAP), 01000 Kangar, Perlis, Malaysia.*
[c]*National Nanotechnology Centre (NNC), Ministry of Science, Technology and Innovation (MOSTI), Federal Government Administrative Centre, 62662 Putrajaya, Malaysia.*
**Corresponding author. Tel.: +603-89118157; fax: +603-89250439; e-mail: ambri@ukm.edu.my*

ABSTRACT

This study reports on DEP-based simulation and experimental validation of polystyrene (PS) beads and fibroblast cells for primary skin cell migration for enhancing wound closure. MyDEP software was used to calculate the numerical simulation of the Clausius-Mossotti factor (CMF). In order to examine particle trajectories based on input frequencies, the finite element technique (FEM) is used. The trajectories of PS beads and fibroblast cells were experimentally assessed to verify the impact of frequency applied on the polarisation of PS beads and fibroblast cells. The outcome illustrated the potential of employing F_{DEP} to move particles and cells to regions of high and low electric field. Fibroblast cells exhibit negative dielectrophoresis (N_{DEP}) at a broad range of frequencies. Thus, F_{DEP} can be utilised for frequency optimisation to enhance wound closure.

Keywords: *Cell Migration, Dielectrophoresis, Electrical stimulation therapy, Wound Healing*

1. INTRODUCTION

Globally, more than 30 million individuals live with diabetes mellitus in 1985. The number of diabetes patient rose to 366 million in 2011 and is projected to reach 552 million by the year 2030 [1,2]. Diabetes slows wound healing by affecting each phase of wound healing, including haemostasis, inflammation, proliferation, and re-modelling [3]. Foot ulcers have been recignised as a clinical marker for limb amputation and mortality in diabetic patients [4,5]. Chronic wounds that take longer to heal may also cause psychiatric stress and depression [6].

Conventional wound treatment procedures include wound dressing [7], wound debridement [8], negative pressure wound therapy [9,10], and hyperbaric oxygen therapy [11]. These procedures are invasive, costly, and time-consuming to show effectiveness. Despite the wide range of treatments alternative, chronic wounds continue to be a significant clinical and economical problem. Therefore, there is a demand for the development of alternative wound healing therapies.

Electrical stimulation therapy (EST) was found to improve healing results in diabetic individuals with open ulcers [12]. EST is a biomimicry approach that replicates the action of endogenous electric field to stimulate and guide cell migration to enhance wound closure [13][14][15]. Fibroblast cell is the main cell in the dermis and plays an important role in skin physiology and wound healing. Kloth et al. demonstrated that exogenously administered electric fields using a DC in mammalian wounds cause fibroblast cell migration toward the cathode, resulting in wound healing. [16]. In this study, we would want to investigate a new approach at the directional fibroblast cell migration based on an electric field gradient for improved wound closure by utilising dielectrophoresis (DEP) technology with an alternating current (AC) supply [15].

Previously, dielectrophoretic-based manipulation has been reported for technology has been applied in various biomedical applications, including, liquid biopsies, stem-cell based therapy, bacterial-related diseased, virus-related diseases, exosomes isolation, cell differentiation, besides DNA and protein manipulations [17–22][23]. DEP allows the elimination of target cell labelling since the manipulation relies on the intrinsic dielectric properties of the cells and medium.

Polystyrene (PS) beads are frequently used as a reference particle in quantitative evaluations of DEP systems to show the feasibility of the device design [22]. PS beads, or artificial particles, are chemically stable and can dissolve in various solvents, buffers, and biological medium. These artificial particles can withstand the strength of an electric field without undergoing significant degradation. Therefore, these artificial particles are used to optimise experimental parameters and validate theoretical models. The Clausius-Mossotti factor (CMF) numerical simulation was computed using MyDEP software. The finite element method (FEM) is used to analyse particle trajectories based on input frequencies. Trajectories of PS beads and fibroblast cells were experimentally evaluated to validate the effect of frequency applied on the polarisation of PS beads and fibroblast cells.

2. THEORY OF DIELECTROPHORESIS

DEP was initially presented in 1951 by Herbert A. Pohl. Pohl defined DEP as an electrokinetic phenomenon for altering the paths of polarisable particles in a non-uniform electric field [5][6]. Particle manipulation by DEP is dependent on the CMF. The real part of the CMF $Re[\tilde{f}_{CM}]$ can be abbreviated in dielectrophoretic force (F_{DEP}) formulation as shown in Equation (1):

$$\langle \vec{F}_{DEP} \rangle = 2\pi\varepsilon_m\varepsilon_0 r^3 Re[\tilde{f}_{CM}]\nabla|\vec{E}|^2 \quad (1)$$

where, ε_o and ε_m represent the permittivity values of vacuum and the relative permittivity of the surrounding medium, the denotes the electric field gradient, the f_{cm} is the Clausius- Mosotti Factor. The F_{DEP} is given by:

$$\tilde{f}_{CM} = \frac{\tilde{\varepsilon}_p - \tilde{\varepsilon}_m}{\tilde{\varepsilon}_p + 2\tilde{\varepsilon}_m} \quad (2)$$

where, $\tilde{\varepsilon}_p$ and $\tilde{\varepsilon}_m$ refer to the complex permittivities of particle and medium, which depend on their respective electrical conductivity and relative permittivity and on the angular frequency, ω and is derived as:

$$\varepsilon^* = \varepsilon - j\frac{\sigma}{\omega} \quad (3)$$

where ε is the permittivity, σ is the electrical conductivity, $j = \sqrt{-1}$ and $\omega = 2\pi f$ where f is the frequency of the applied field.

Based on the CMF, particle can be manipulated towards high electric field strength or low electric field strength. Positive dielectrophoresis (P_{DEP}) occurs when particles are manipulated towards high electric field strength, while negative dielectrophoresis (N_{DEP}) occurs when particles are manipulated towards low electric field strength. The crossover frequency (f_{xo}) is the frequency at which particles transition between N_{DEP} and P_{DEP} [26][27].The schematic diagram of P_{DEP} and N_{DEP} are as depicted in figure 1.

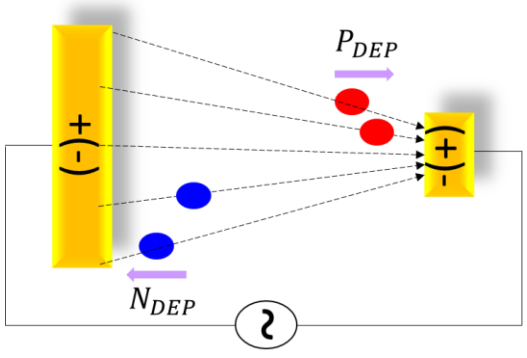

Figure 1. Schematic illustration of positive dielectrophoresis (P_{DEP}) and negative dielectrophoresis (N_{DEP}).

3. MATERIALS AND METHODS

3.1. Materials

Fluorescence PS beads (Thermo Fisher Scientific, Fremont, CA, USA) with the size of 15 µm were used for as a standard particle for DEP manipulation. The PS Beads were diluted in de-ionised (DI) water to produce sample with 5.0 × 10^5 particle/mL. Human dermal fibroblast (HDF) cells which was extracted from the skin tissue of consented patient were cultured in 75 cm^2 T-flask and placed in the incubator at 37 °C in an atmosphere of 95 % air and 5% CO_2. The cultured cells suspended in Dulbecco's Modified Eagle's Medium (DMEM) with 10% foetal bovine serum (F12:DMEM) (1:1, Sigma Aldrich, USA) (PAA Laboratories, Austria) were utilised for DEP manipulation.

3.2. Numerical Simulation: The Clausius Mosotti Factor

MyDEP is a standalone software (v1.0.1) developed by Cottet et. al [28]. MyDEP is a Java program that analyzes the electrical characteristics of living cells and studies the reaction of dielectric particles to AC electric fields [29]. The CMF number represents the magnitude and direction of theF_{DEP}. PS beads are homogeneous spherical particle [30], while fibroblast cells are regarded as inhomogenous single shell sphere [31][20]. Homogenous single shell sphere represents a cell consisting of a spherical core cytoplasm and outer cell membrane. The dielectric properties of PS beads, fibroblast cells and suspension medium utilised in this study is as tabulated in Table 1.

3.3. Numerical Simulation: Finite Element Method

The trajectories of PS beads and fibroblast cells were computed using the FEM, COMSOL Multiphysics® 5.6 software. The FEM study was conducted using a simplified tapered microelectrode array (TAMA) configuration. [32][33]. Two key steps in the simulation study are required to establish particle trajectories. By linking the solution from Study 1 (electric current and laminar flow) and study 2 (particle tracing for fluid flow), the particle trajectory was developed.. In Study 1, the electrical potential is described by electric current, which is calculated in the frequency domain (AC). The coupling was accomplished by connecting the frequency domain solution of Study 1 to the particle trajectory solution of Study 2 with time-dependent study to support the analysisThe electrical potential of V_0 was set to +7V and - 7 V, (14 V_{pp}), is defined by electric current in a frequency domain (AC).

3.4. DEP Microelectrode Platform

Tapered microelectrode array (TAMA) was fabricated on a pre-cleaned silicon substrate by photolithography method [29][33][34][35][36]. Silicon oxide (SiO_2) layer with thickness of 1.15 µm were grown on silicon (Si) substrate by plasma enhanced chemical vapour deposition process. Then, titanium (Ti)/titanium nitrite (TiN) thin film with a thickness of 60/30 nm was deposited as an adhesion layer through physical vapour deposition . Subsequently, a 4.0 µm-thick layer of aluminum (Al), silicon (Si), and copper (Cu) was deposited via physical vapour deposition (PVD).

For electrode patterning, a layer of photoresist was applied to the substrate and then subjected to ultraviolet (UV) radiation. Reactive ion etching (RIE) was performed to remove undesired metal and produce a tapered electrode profile. The gap between the metal contact pads is 80 µm.

Table 1 Dielectric properties of polystyrene beads, fibroblast cells and suspension medium.

Particles/Cell/Medium	Particle/Cell Model	Diameter	Electrical Conductivtiy, σ_p (S/m)	Electrical Permittivity, ε_p
Polystyrene (PS) beads [30]	Homogeneous sphere	15 µm	5.33 x 10^4	2.55
De-ionised (DI) water	-	-	1.68 x 10^4	78.5
Fibroblast cells [31]	Homogeneous single shell sphere	Cell diameter = 15 µm	Cytoplasm : 0.6	Cytoplasm : 50 x ε_o
		Membrane thickness= 0.006 µm	Membrane :1 x 10^6	Membrane : 12 x ε_o
Dulbecco's Modified Eagle's Medium (DMEM) with 10% foetal bovine serum (F12:DMEM)	-	-	2.072	80

*Permittivity of free space, ε_o = 8.854 x 10^{-12} Fm^{-1}

3.5. Experimental Set-Up

An optical microscope (OLYMPUS - BX53M Upright Microscope) is used to observe the manipulation of PS particles and HDF. The microscope was mounted with a digital high-speed camera (HAS-D71, DITECT Corporation, Japan) and connected to a computer with HAS-XViewer software (Ver.1.3.5.0.) to monitor and record cell trajectories with a capturing speed of 500 frame per second (fps).The probe is positioned on the metal contact of the TAMA and is connected to a function generator (Teledyne LeCroy-WaveStation) . To visualize the F_{DEP} behavior, approximately 10 µL of HDFs sample were dropped on the ROI to energise the micro-electrodes. Micro cover glass with a size of 20 x 20 mm was placed on the ROI of the micro-electrode to disperse the sample. Particle and cell trajectories were examined at a 50x magnification. The trajectories were analysed between 80 kHz to 1 MHz, with 10 kHz and 100 kHz increment, and 100 kHz increment between 100 kHz to 1 MHz, respectively. The manipulation is monitored and recorded using HAS-XViewer software .

4. RESULTS AND DISCUSSION

4.1. Clausius-Mossotti Factor

The graph of CMF vs frequency for 15 µm PS beads in DI water and fibroblasts cells in DMEM are shown in Figure 2. Above zero baselines in this graph indicate P_{DEP}, while below zero baseline indicate N_{DEP}. The CMF of PS beads shows that the crossover frequency (f_{xo}) of 15 µm PS bead is at 91.73 kHz. This indicates that below this frequency, PS beads exhibit P_{DEP}, and above this frequency, PS beads exhibit N_{DEP}. Meanwhile, fibroblast cell exhibit N_{DEP} at all frequencies. DI water was used as suspension medium for polystyrene (PS) beads. Meanwhile, biological aqueous medium, the Dulbecco's Modified Eagle's Medium (DMEM) with 10% foetal bovine serum (F12:DMEM) was used as the suspension medium for the fibroblast cells as cells has low viability in DI water [37].

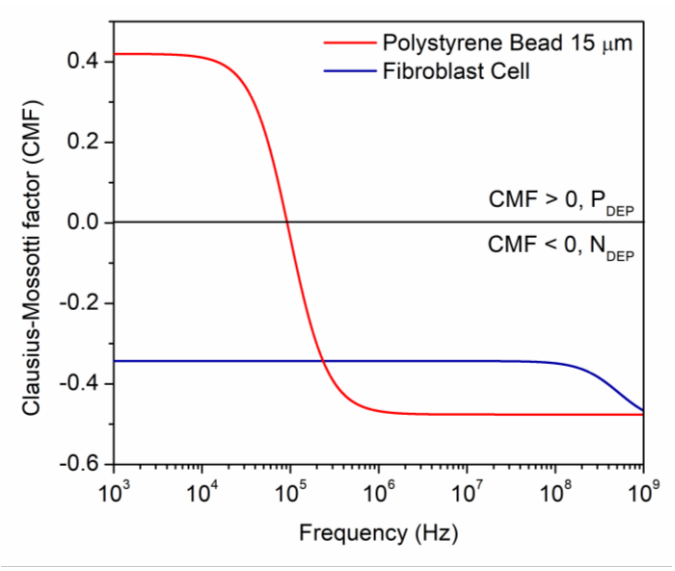

Figure 2. The CMF of PS beads and fibroblast cells in suspending medium.

4.2. FEM of Polystyrene Beads and Fibroblast Cells

Figure 3 shows the trajectories of 15 µm PS beads. Figure 3a shows the initial states of the particle. Figure 3b shows the trajectories of the particle at 90 kHz after 10 sec. At 90 kHz, PS beads move to the electrode edge, a high electric field region, indicating P_{DEP}. Figure 3c shows that at 400 kHz, PS beads move to low electric field region, indicating that PS beads exhibit N_{DEP} at 400 kHz.

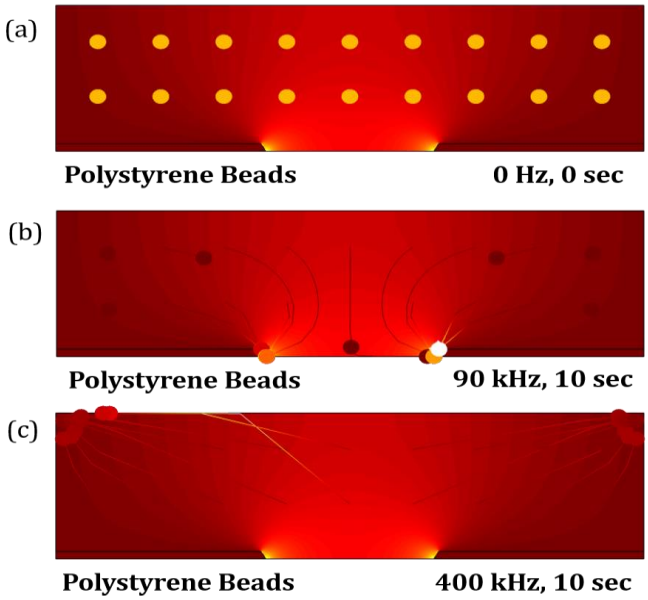

Figure 3. The trajectories of PS beads at (a) 0 sec, (b) 90 kHz (P_{DEP}) and (c) 400 kHz (N_{DEP}).

Figure 4 shows the trajectories of fibroblast cell. Figure 4a shows the initial states of the particle. Figure 4b shows the trajectories of the particle at 90 kHz after 10 sec. At 90 kHz, fibroblast cell move to the low electric field region, indicating N_{DEP}. Figure 4c shows that at 1 MHz, fibroblast move to low electric field region, indicating N_{DEP}.

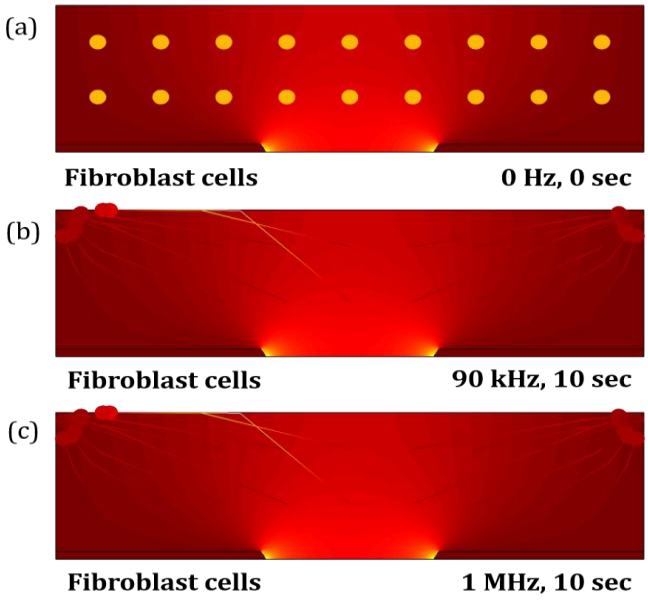

Figure 4. The trajectories of fibroblast cell at (a) 0 sec, (b) 90 kHz (N_{DEP}), and (c) 1 MHz (N_{DEP}).

4.3. Experimental Validation of Dielectrophoretic Effect

Based on our findings, the input frequency affects the trajectories of the PS beads at the region of interest (ROI). Figure 5a shows the initial position of PS beads. After 7 sec, 90 kHz, there is no PS beads left at the ROI as shown in Figure 5b. This shows that the PS beads move to towards the electrode with high electric field, indicating that PS beads experience P_{DEP}.

Figure 5c shows the initial position of PS beads. After 10 sec, 400 kHz, PS beads move to the low electric field region. This indicate that PS beads experience N_{DEP}. This study shows the feasibility of the electrode to generate both P_{DEP} and N_{DEP}. Figure 5e show the initial position of fibroblast cells. At 14 V_{pp}, 90 kHz, fibroblast cells move low electric field region. This indicate that fibroblast cells experience N_{DEP}. The same effect was observed at 1 MHz, as shown in Figure 5h.

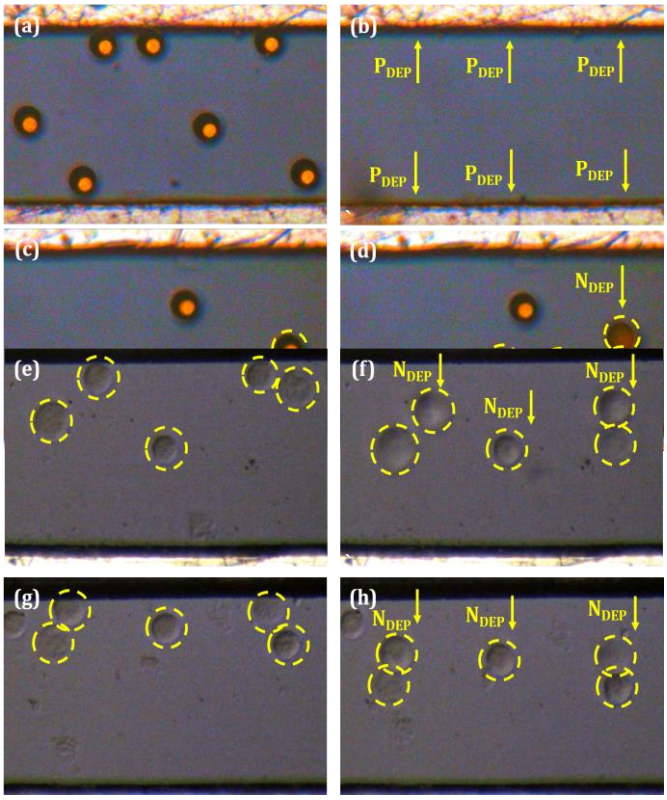

Figure 5. Image of (a) position of PS beads at 0 sec, (b) position of PS beads after 7 s at 90 kHz. The image shows no PS beads left at the ROI after 10 sec indicating P_{DEP}, (c) position of PS beads at 0 sec, (d) position of PS beads after 10 sec at 400 kHz, indicating N_{DEP}, (e) position of fibroblast at 0 sec, (f) position of fibroblast after 10 s at 90 kHz, indicating N_{DEP}, (g) position of fibroblast at 0 sec, (h) position of fibroblast after 10 s at 1 MHz kHz, indicating N_{DEP}.

5. CONCLUSION

In this work, we have demonstrated the feasibility of using F_{DEP} to migrate particles and fibroblast cells to high and low electric field region. Since fibroblast cells, which is a primary skin cell exhibit negative dielectrophoresis (N_{DEP}) at a broad range of frequencies, F_{DEP} can be utilised for frequency optimisation to enhance wound closure.

ACKNOWLEDGMENTS

This research was financially supported by the Transdisciplinary Research Grant Scheme (TRGS) under the grant number of TRGS/1/2019/UKM/02/1/1 form the Ministry of Higher Education (MOHE) Malaysia. The authors would also like to thank all the team members in Centre for Tissue Engineering and Regenerative Medicine (CTERM),

Universiti Kebangsaan Malaysia Medical Centre for their guidance and assistance in the cell culture process.

REFERENCES

[1] J. E. Shaw, R. A. Sicree, P. Z. Zimmet, Global estimates of the prevalence of diabetes for 2010 and 2030, Diabetes Res. Clin. Pract. 87 (2010) 4–14. https://doi.org/10.1016/j.diabres.2009.10.007.

[2] D. R. Whiting, L. Guariguata, C. Weil, J. Shaw, IDF Diabetes Atlas : Global estimates of the prevalence of diabetes for 2011 and 2030, Diabetes Res. Clin. Pract. 94 (2011) 311–321. https://doi.org/10.1016/j.diabres.2011.10.029.

[3] L. Martınez-Santamaria, C. J. Conti, S. Llames, E. Garcia, L. Retamosa, M. Del R, F. Larcher, A. Meana, The regenerative potential of fibroblasts in a new diabetes-induced delayed humanised wound healing model, Exp. Dermatol. (2013) 195–201. https://doi.org/10.1111/exd.12097.

[4] M. M. Iversen, G. S. Tell, T. Riise, B. R. Hanestad, T. Østbye, M. Graue, K. Midthjell, History of Foot Ulcer Increases Mortality, Diabetes Care. 32 (2009). https://doi.org/10.2337/dc09-0651.

[5] D. Martins-Mendes, M. Monteiro-Soares, E.J. Boyko, M. Ribeiro, P. Barata, J. Lima, R. Soares, The independent contribution of diabetic foot ulcer on lower extremity amputation and mortality risk, J. Diabetes Complications. 28 (2014) 632–638. https://doi.org/10.1016/j.jdiacomp.2014.04.011.

[6] R. Renner, C. Erfurt-Berge, Depression and quality of life in patients with chronic wounds: ways to measure their influence and their effect on daily life, Chronic Wound Care Manag. Res. (2017) 143–151.

[7] E. Gianino, C. Miller, J. Gilmore, Smart wound dressings for diabetic chronic wounds, Bioengineering. 5 (2018). https://doi.org/10.3390/bioengineering5030051.

[8] D. C. Thomas, C. L. Tsu, R. A. Nain, N. Arsat, S. S. Fun, N. A. Sahid Nik Lah, The role of debridement in wound bed preparation in chronic wound: A narrative review, Ann. Med. Surg. 71 (2021) 102876. https://doi.org/10.1016/j.amsu.2021.102876.

[9] Z. Li, A. Yu, Complications of negative pressure wound therapy: A mini review, Wound Repair Regen. 22 (2014) 457–461. https://doi.org/10.1111/wrr.12190.

[10] K. Shimada, Y. Ojima, Y. Ida, T. Komiya, H. Matsumura, Negative-pressure wound therapy for donor-site closure in radial forearm free flap: A systematic review and meta-analysis, Int. Wound J. 19 (2022) 316–325. https://doi.org/10.1111/iwj.13632.

[11] S. Liu, C. zhu He, Y. ting Cai, Q. ping Xing, Y. zhen Guo, Z. long Chen, J. liang Su, L. ping Yang, Evaluation of negative-pressure wound therapy for patients with diabetic foot ulcers: Systematic review and meta-analysis, Ther. Clin. Risk Manag. 13 (2017) 533–544. https://doi.org/10.2147/TCRM.S131193.

[12] L. L. Baker, R. Chambers, S. K. DeMuth, F. Villar, Healing in Patients With Diabetic Ulcers, Diabetes Care. 20 (1997) 405–412.

[13] M. Rouabhia, H. Park, S. Meng, H. Derbali, Z. Zhang, Electrical stimulation promotes wound healing by enhancing dermal fibroblast activity and promoting myofibroblast transdifferentiation., PLoS One. 8 (2013). https://doi.org/10.1371/journal.pone.0071660.

[14] M. Zhao, J. Penninger, R.R. Isseroff, Electrical Activation of Wound-Healing Pathways., Adv. Skin Wound Care. 1 (2010) 567–573. https://doi.org/10.1089/9781934854013.567.

[15] N. N. Mohd Maidin, R. Deivasigamani, M. R. Buyong, N. A. M. Som, M. A. Mohamed, Chapter 6: Wound Healing Utilising Electrical Stimulation Technique: Towards Application of Dielectrophoresis, in: Funct. Bio-Based Mater. Regen. Med. From Bench to Bedsite-Part 1, 2023: p. 96.

[16] L. C. Kloth, Electrical stimulation for wound healing: A review of evidence from in vitro studies, animal experiments, and clinical trials, Int. J. Low. Extrem. Wounds. 4 (2005) 23–44. https://doi.org/10.1177/1534734605275733.

[17] S. D. Ibsen, J. Wright, J. M. Lewis, S. Kim, S. Ko, J. Ong, S. Manouchehri, A. Vyas, J. Akers, C. C. Chen, B. S. Carter, S. C. Esener, M. J. Heller, Rapid Isolation and Detection of Exosomes and Associated Biomarkers from Plasma, ACS Nano. (2017). https://doi.org/10.1021/acsnano.7b00549.

[18] L. Shi, D. Kuhnell, V. J. Borra, S. M. Langevin, T. Nakamura, L. Esfandiari, Rapid and label-free isolation of small extracellular vesicles from biofluids utilizing a novel insulator based dielectrophoretic device, Lab Chip. 19 (2019) 3726–3734. https://doi.org/10.1039/c9lc00902g.

[19] S. Li, Z. Ye, Y. S. Hui, Y. Gao, Y. Jiang, W. Wen, On-chip DNA preconcentration in different media conductivities by electrodeless dielectrophoresis, Biomicrofluidics. 9 (2015). https://doi.org/10.1063/1.4932177.

[20] N. N. Mohd Maidin, M. R. Buyong, R. A. Rahim, M. A. Mohamed, Dielectrophoresis applications in biomedical field and future perspectives in biomedical technology, Electrophoresis. 42 (2021) 2033–2059. https://doi.org/10.1002/elps.202100043.

[21] B. Sarno, D. Heineck, M. J. Heller, S. D. Ibsen, Dielectrophoresis: Developments and applications from 2010 to 2020, 2021. https://doi.org/10.1002/elps.202000156.

[22] Q. Chen, Y. J. Yuan, A review of polystyrene bead manipulation by dielectrophoresis, (2019) 4963–4981. https://doi.org/10.1039/c8ra09017c.

[23] N. S. Abdul Nasir, R. Deivasigamani, M. F. Mohd Razip Wee, A. A. Hamzah, M. H. Mat Zaid, M. K. Abdul Rahim, A. Ahmad Kayani, A. Abdulhameed, M. R. Buyong, Protein Albumin Manipulation and Electrical Quantification of Molecular Dielectrophoresis Responses for Biomedical Applications, Micromachines. 13 (2022) 1–22. https://doi.org/10.3390/mi13081308.

[24] H. A. Pohl, Some effects of nonuniform fields on dielectrics, J. Appl. Phys. 29 (1958) 1182–1188. https://doi.org/10.1063/1.1723398.

[25] H. A. Pohl, The Motion and Precipitation of

Suspensoids in Divergent Electric Fields, J. Appl. Phys. 22 (1951) 10–13. https://doi.org/10.1063/1.1700065.

[26] M. Li, R. K. Anand, High-Throughput Selective Capture of Single Circulating Tumor Cells by Dielectrophoresis at a Wireless Electrode Array, J. Am. Chem. Soc. 139 (2017) 8950–8959. https://doi.org/10.1021/jacs.7b03288.

[27] M. K. Abdul Rahim, N. M. A. Jamaludin, J. Santhanam, A. A. Hamzah, M. R. Buyong, Rapid ESKAPE pathogens detection method using tapered dielectrophoresis electrodes via crossover frequency analysis, Sains Malaysiana. 49 (2020) 2913–2925. https://doi.org/10.17576/jsm-2020-4912-04.

[28] J. Cottet, O. Fabregue, C. Berger, P. Renaud, MyDEP : A New Computational Tool for Dielectric Modeling of Particles and Cells, (2019) 1–7. https://doi.org/10.1016/j.bpj.2018.11.021.

[29] M. R. Buyong, F. Larki, M. S. Faiz, A. A. Hamzah, J. Yunas, B. Y. Majlis, A tapered aluminium microelectrode array for improvement of dielectrophoresis-based particle manipulation, Sensors (Switzerland). 15 (2015) 10973–10990. https://doi.org/10.3390/s150510973.

[30] T. Honegger, K. Berton, E. Picard, D. Peyrade, Determination of Clausius-Mossotti factors and surface capacitances for colloidal particles, Appl. Phys. Lett. 98 (2011) 2011–2014. https://doi.org/10.1063/1.3583441.

[31] S. H. Ling, Y. C. Lam, K. S. Chian, Continuous cell separation using dielectrophoresis through asymmetric and periodic microelectrode array, Anal. Chem. 84 (2012) 6463–6470. https://doi.org/10.1021/ac300079q.

[32] R. Deivasigamani, N. N. Mohd Maidin, M. F. Mohd Razip Wee, M. A. Mohamed, M. R. Buyong, Dielectrophoresis Prototypic Polystyrene Particle Synchronization toward Alive Keratinocyte Cells for Rapid, Sensors. 21 (2021). https://doi.org/10.3390/s21093007.

[33] M. R. Buyong, F. Larki, C. E. Caille, Y. Takamura, A. A. Hamzah, B. Y. Majlis, Determination of lateral and vertical dielectrophoresis forces using tapered microelectrode array, Micro Nano Lett. 13 (2018) 143–148. https://doi.org/10.1049/mnl.2017.0542.

[34] M. R. Buyong, A. A. Kayani, A. A. Hamzah, B. Y. Majlis, Dielectrophoresis manipulation: Versatile lateral and vertical mechanisms, Biosensors. 9 (2019). https://doi.org/10.3390/bios9010030.

[35] M. R. Buyong, F. Larki, Y. Takamura, B. Yeop Majlis, Tapered microelectrode array system for dielectrophoretically filtration : fabrication, characterization, and simulation study, J. Micro/Nanolithography, MEMS MOEMS. (2017). https://doi.org/10.1117/1.JMM.16.4.044501.

[36] N. N. Mohd Maidin, R. A. Rahim, M. H. Jacho, N. H. A. Halim, A. S. Z. Abidin, N. A. Ahmad, Fabrication of graphene-based back-gated field effect transistor for cortisol detection, Int. J. Nanoelectron. Mater. 11 (2018) 123–128.

[37] R. Deivasigamani, N. N. Mohd Maidin, N. S. Abdul Nasir, A. Abdulhameed, A. Bin Ahmad Kayani, M. A. Mohamed, M. R. Buyong, A correlation of conductivity medium and bioparticle viability on dielectrophoresis-based biomedical applications, Electrophoresis. 44 (2023) 573–620. https://doi.org/10.1002/elps.202200203.